ACCESSIBILITY

OsloMet – Oslo Metropolitan University

Department of Civil Engineering & Energy Technology
Section of Civil Engineering

Master Program in Structural Engineering & Building Technology

MASTER THESIS

TITLE OF REPORT	DATE
Installation analysis of a long floating pontoon bridge	25.05.2023
	PAGES / ATTACHMENTS 39/9
AUTHOR(S) Tord Rønning Lalesh Bero	SUPERVISOR(S) Jian Dai

IN COLLABORATION WITH	CONTACT PERSON
Statens Vegvesen	Xu Xiang

SUMMARY / SYNOPSIS

The Norwegian ferry free E39 project aims to cut the current travel time by half from Kristiansand in the south to Trondheim in the north. Crossing the Bjørnafjord, investigated in this thesis, using conventional pier bridge designs is unfeasible. One possible solution to this problem is a floating pontoon bridge. Pontoon bridges can divide a bridge over water into several smaller bridge spans, reducing the required capacity and therefore the size and weight of the bridge. Subsequently, it is important to determine the suitable bridge segmentation and environmental windows for onsite installation and connection.

Numerical analysis on a long floating bridge gave knowledge of the hydrodynamic behavior of bridge segments under different environmental conditions. Perpendicular wave directions induce more moments in the bridge girder, compared to parallel waves. When increasing the wave height from 0,2 to 0,35 and then 0,5 meters there is <1% change in peak moments about the horizontal axis. However, the moments about the vertical axis increase by 200%. The paperwork also shows the effect of wave heights on the strong axis bending being more dominating, however the values in general are low compared to the structural capacity.

KEYWORDS
Hydrodynamic
Bridge segment
Installation

Preface

Our journey writing the master thesis during the spring semester of 2023 was turbulent but ultimately instructive. For some of us, floating bridge construction and hydrodynamics were completely new fields of study. However, our desire to understand and explore the latest transport and construction solutions such as floating pontoon bridges drove us forward. Through careful research, analysis, and discussion over the course of five months, we eventually grew wiser in these fields and became aware of the complexities of the system.

We acknowledge and thank our internal supervisors, Associate Professor Jian Dai from the department of Civil Engineering and Energy Technology at Oslo Metropolitan University, for providing us with help, guidance, and motivation throughout our journey. We would also like to express our appreciation to Xu Xiang, Chief Engineer for Complex Constructions in Statens Vegvesen, for the resources provided that enabled us to put together this thesis, as a part of our final course MABY5900 at Oslo Metropolitan University.

Sincerely,
Tord Rønning and Lalesh Bero

Table of Contents

List of figures

List of tables

1 Introduction

Bridges are vital for economic growth by allowing transportation of resources, people and industry over rivers, fjords, valleys and lakes. Conventional bridges rely on piers standing on firm foundation to distribute loads and remain stable. Bridges built over water use piers with wide feet that are fixed to the solid rock in or under the seabed. When seabed conditions are soft, with deep and wide fjords, the construction of conventional piers becomes increasingly challenging and more expensive.

Crossing the Bjørnafjord, investigated in this thesis, using conventional pier bridge designs is unfeasible. The 5-kilometer-wide fjord has soft undulating seabed conditions and is over 100 meters deep (Statens Vegvesen, 2017). Constructing a suspension bridge capable of spanning 5 kilometers would be more than double the world's longest current bridge span. One possible solution to this problem is a floating pontoon bridge. Pontoon bridges can divide a bridge over water into several smaller bridge spans, reducing the required capacity and therefore the size and weight of the bridge. Long span floating bridges rely on the natural buoyancy of pontoons to support the payload in the gravitational direction and use deep water mooring lines to limit the horizontal motions. An added benefit of floating bridges is the possibility of transporting large complete sections of bridge over sea by towboats, utilizing the self-buoyancy of the structure.

During construction in highly populated or heavy traffic areas bridges are divided and built in a specific order to reduce the impact of large building projects and due to the limited capacity of construction yards. It can be difficult and expensive to reroute traffic around the construction site for long periods of time, and as a solution engineers can designate an order of operations for a project. Prefabricated concrete bridge segments can be constructed off site and transported in to reduce the time a road must stay closed during concrete casting. For floating structures like oil platforms, the massive concrete structures are cast on land before being towed to the final location at sea. Floating bridges require significant infrastructure during construction, and creating temporary docks for welding of pontoons and quality checking could be expensive and environmentally damaging to surrounding areas. It is therefore important to evaluate the stability and motions of truncated self-buoyant bridge sections and assess the hydrodynamic performance under various environmental conditions to open the possibility of transporting complete prefabricated sections of the superstructure.

As the Earth's population continues to increase, and sea levels continue to rise, it is vital to facilitate the use of islands and fjords. As explained in the book *Very Large Floating Structures* "There is need for a sustainable and environmentally friendly development. Technological

innovations that promote stewardship of the Earth's resources, especially the ocean, are vital for mankind's survival in the next millennium.» (Wang & Tay, 2007).

1.1 Background

The Norwegian ferry free E39 project aims to cut the current travel time by half from Kristiansand in the south to Trondheim in the north. Currently the coastal road uses several ferry connections to cross fjords that otherwise would take hours to drive around. One of the wider fjords is the Bjørnafjorden crossing (figure 1). Multiple >4km long floating bridge designs have been proposed by several companies. One of the proposed designs is from a group of large consulting firms, led by Multiconsult, and will be the main resource used during modelling and analysis in this thesis (Statens Vegvesen, 2017).

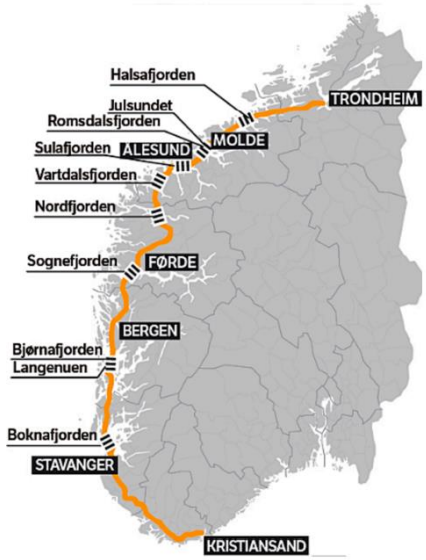

Figure 1: E39 costal highway route (Hove et al., 2015)

In the early phases of this thesis the focus of the group was to increase our understanding of hydrodynamic responses and especially wave interaction with floating structures. A literature study was conducted but there was little available information regarding large floating structures. We expect this is due to a combination of factors, as floating bridges are both rare and as a relatively new research topic there is simply not enough information available. Because these projects often are incredibly extensive and resource intensive the contracts go to the largest companies. These companies don't have an incentive to share their knowledge as that would

allow other companies to learn from their mistakes and compete better. Due to the lack of resources available a chain search using authors from the initial literature search was then conducted.

Significant research and engineering design works have been conducted by several parties regarding the design and development of the Bjørnafjorden crossing. Multiconsult has directly or through sub-contractors done analysis regarding statics, Environmental loads, Global response, Aerodynamics, Robustness and sensitivity analyses (Statens Vegvesen, 2017). The process of designing pontoons, girders, columns, abutments, mooring lines, anchorages and the high bridge section has been documented thoroughly. In addition, the effects of various complex environmental conditions on the structural responses of the design concepts have been investigated. For example, J. Dai examined the effects of wave inhomogeneity on a long straight side anchored floating bridge model based on the Bjørnafjorden crossing by Multiconsult (Dai et al., 2020). Later Dai investigated the effects of wave-current interaction on a curved version of the Bjørnafjorden bridge design (Dai et al., 2022). The extreme responses of the Bjørnafjorden crossing has been researched based on the MetOcean design basis also used in this thesis (Cui et al., 2023). Numerical simulations have been conducted to investigate the bridge response to a ship collision, with good results compared to a cruise ship (Sha et al., 2017).

Despite significant research into several properties in similar Bjørnafjord models, something that has remained largely unchanged has been the on-site assembly. The installation method explained by Multiconsult uses prefabricated bridge elements from Europe or Asia that are assembled into larger bridge segments in a nearby fjord before being towed to their final location. A wind wave analysis was conducted by a group of consulting firms to determine significant wave heights and directions along the proposed towing route for the prefabricated elements (Norconsult, 2019).

Prefabrication is a widely used practice when constructing large structure projects like bridges. By transporting prefabricated bridge sections, it is possible to lower costs, increase quality assurance, and reduce the requirements for large on-site temporary structures for welding and assembly. Transporting floating bridge deck segments for bridges can be done using barges, where the segments are hoisted using cables from the water surface up to the bridge deck height. While prefabrication of bridge elements has proven to be an effective way of lowering costs, floating bridges also introduce the possibility of transporting complete bridge sections.

One example of the effectiveness of transportation of floating bridge structures is the Yumemai Bridge in Japan. Yumemai bridge is a pontoon supported, steel arched, highway bridge, spanning 135 meters with a swing mechanism to allow for ship passage. Both bridge abutments were

constructed on site, and the main span pontoon bridge was built off site. The bridge was constructed in a dry dock about 10 km away, before being towed to its final location (figure 2). Construction of the bridge took over 2 years, but the installation of the bridge only took one day (Maruyama & Kawamura, 2000, p. 39; Watanabe et al., 2000).

Figure 2: Towing of a floating bridge segment (Maruyama & Kawamura, 2000)

Large floating bridge projects are rare, and as such there is little literature available directly related to these projects. Some of the largest floating bridges in the world have had postponements and increases in costs due to excessive cost cutting and unforeseen complications. Creating large new structures such as docks and ports to use temporarily during construction increases the possibility of failure or setbacks that could eventually affect the main structure.

Hood Canal Bridge located in Washington state needed repair and refurbishment on 14 of its concrete pontoons. Washington State Department of Transportation had planned to purchase a local dock to use during construction of replacement pontoons. Just 10 days after the project started the site was deemed to be of significant historical significance as it had formally been a Native American burial site. In total this postponed the project by 18 months (Wilma & Oldham, 2005).

The Nordhordlands Bridge was completed in 1994 (figure 3), it was the longest floating bridge at the time in Europe and spans 500m deep, over 1,5 km wide fjord north of the city of Bergen. Individual parts of the bridge were constructed across the country in Fredrikstad, before they were transported and assembled in Lonevåg about 15 km away from the bridge site. Using towboats the completed 1km long bridge was towed in early July, less than three months before

the bridge opened to the public (Moe, 1995). This three-step assembly consists of: Construct small sections, connect sections into large sections of bridge, on-site assembly of complete bridge, cuts down on the impact large projects have on the environment and on local wildlife.

Figure 3: Nordhordlandsbrua (Wikipedia, 2023)

Transporting bridge sections further could allow construction in bigger, more qualified locations compared to local construction. Quality assurance is a necessary step to discover errors or mistakes early in the process, as economics of scale push the construction industry to cut corners, QA can reduce the impact those errors incur. If significant faults are found late in the construction process the costs of repair and postponement go up significantly. The Albert D. Rosellini Evergreen Point Floating Bridge had trouble with cracks in prefabricated pontoons during assembly that led to increased costs and significant loss of time (Douglas, 2013).

As floating bridges are sophisticated and complex structures, there are a limited number of realized projects and thus rather limited information available when compared to the traditional bottom funded counterpart. Currently floating bridges are used mainly to cross spans where traditional bridges are too expensive or border on impossible to construct. When it comes to very

long floating bridges such as the proposed project for crossing Bjørnafjorden, it is even more challenging, and one must examine the reliability of relevant knowledge and experience for constructing and installing similar structures. Increasing the knowledge regarding installing long floating bridges could determine whether floating bridges could replace some traditional bridges due to the practicality of construction-connect-assemble and the possibility of relocation during repairs or demolition.

1.2 Motivation

Although there is significant documentation regarding the construction of traditional bridges, there is little information about floating bridges, especially very long floating bridges. The possibility of constructing large sections of the superstructure in already established industrial areas and later towing them to location could save significant cost, resources, time and environmental impact. However, for long and very long floating bridges, it is important to determine the suitable bridge segmentation and environmental windows for onsite installation and connection. This requires knowledge of the hydrodynamic behavior of bridge segments under different environmental conditions.

1.3 Objective

The objective of this thesis is to investigate the hydrodynamic performances of a truncated floating bridge segment under various wave conditions. This thesis considers the long floating bridge based on the design proposed by Statens Vegvesen and Multiconsult. The hydrodynamic properties of a pontoon are analyzed in the frequency domain using the commercial boundary element based potential flow solver HydroD, then the hydrodynamic responses of bridge segments using the time domain solver SIMA. Detailed parametric studies are conducted to examine the effect of different wave conditions and hydrodynamic performance of the bridge segment. Recommendations on suitable environmental window are given based on the findings of the detailed study.

1.4 Layout

The thesis is arranged as follows. Chapter 1 introduces the concept of floating bridges as well as the motivation and objective of this study. Chapter 2 details the model and the methodology used in the study. Chapter 3 details the analysis of the bridge segment under various wave heights

from different directions. Finally, the conclusions and recommendations for future work are summarized in chapter 4.

2 Methodology and models

2.1 Model definition

This study is based on a comprehensive bridge design proposed by a group of consulting firms led by Multiconsult and Statens Vegvesen as illustrated in figure 4. The bridge design is a very long floating pontoon bridge which consists of a cable-stayed bridge section in the south that allows for ship passage and a floating pontoon section in the north. The floating bridge is side anchored and uses four groups of deep-water mooring lines to restrain the transverse motion of the bridge. Pontoons are spaced about 125 meters apart, connected by a box girder 18 meters above the water surface. The box girder will carry four lanes of traffic as well as one pedestrian lane. The pontoons, columns and girders are all made from structural steel. Between pontoons the thickness of the girder tapers, which results in a reduction of strength. To more accurately represent this, the model uses two girder sections as shown in figure 5. The chosen pontoon geometry is shown in figure 6.

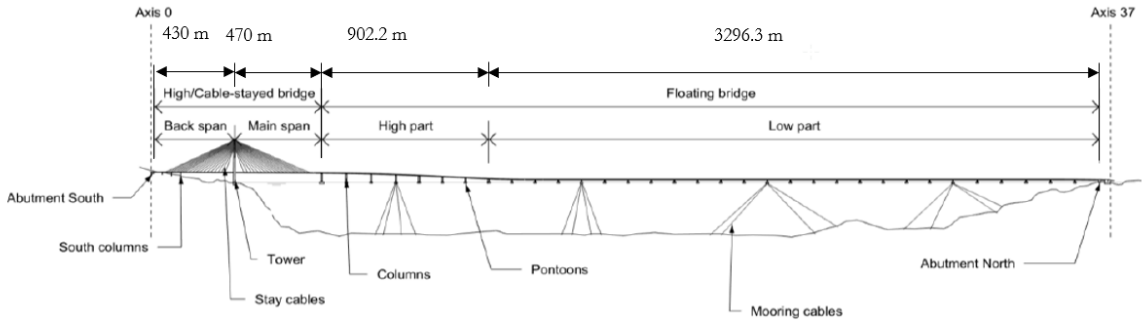

Figure 4: View of bridge from east (Statens Vegvesen, 2017)

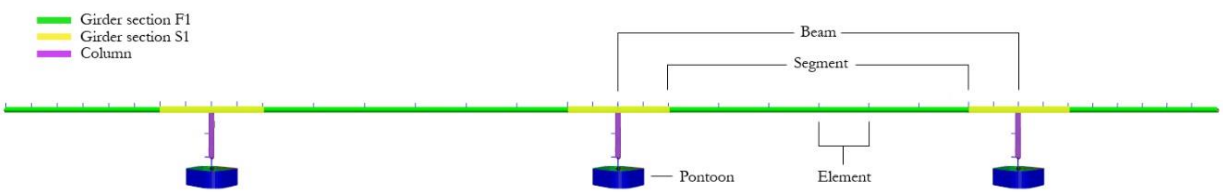

Figure 5: Idealization of bridge

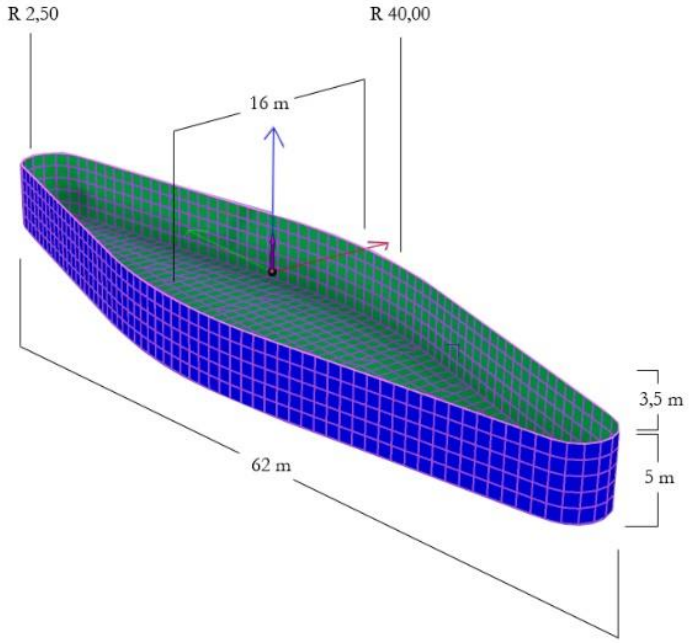

Figure 6: Pontoon geometry with 5m draft and 3,5m freeboard

This study focuses on the elevated floating pontoon bridge in the north, using the pontoon design shown in figure 6. The simplified 375m long truncated floating bridge (figure 5) is elevated 18 meters above the water surface, moored at the outermost pontoons for horizontal transverse motion. The water depth is set to 300 meters and is assumed to be constant throughout the fjord. According to Cheng and his collaborators the impact of varying water depth is mostly in the low frequencies, and thus the effect can be seen as negligible on the dynamic responses of the bridge (Zhengshun et al., 2018). As a result, the water depth is set according to the floating bridge model presented by (Dai et al., 2022). The columns and girders are modelled as Euler-Bernoulli beams, while the pontoons are regarded as rigid bodies interacting with water.

Table 1: Bridge sectional properties

Section	Mass (kg/m)	Sectional area (m^2)	I_x (m^4)	I_y (m^4)	I_z (m^4)	I_{xx} (m^4)
Girder S1	19780	1.65	116.52	7.88	4.06	1.3×10^6
Girder F1	16040	1.17	89.88	6.64	3.21	1.1×10^6
Column	9180	1.53	12.94	14.92	9.65	2.3×10^5

Table 2: Pontoon properties

Freeboard (m)	Draft (m)	Mass (ton)	Planar area (m^2)	Radius of gyration		
				r_x (m)	r_y (m)	r_z (m)
3.5	5.0	850	667	16.1	5.2	16.3

The structural bridge components are modelled as three-dimensional prismatic Euler-Bernoulli beam elements using the finite element method.

Due to a combination of yield strength criteria, cost savings and resistance to erosion with the seabed a combination of materials are used for mooring lines. The lines are divided into three parts, where the first 50-meter and final 100-meter segments are studless chains built for marine environments. The main middle part of the chain is a wire with significantly lower mass, but with a higher axial stiffness. To simplify the modelling of mooring lines a spring support is added at both outermost pontoons. The spring support limits horizontal movement but allows for vertical movement and rotation around all axes. The equivalent mooring cluster spring stiffnesses are derived from the restoring curves of the mooring clusters and employed in the numerical model in this study.

The bridge girder is modelled as two distinct sections, one stronger section 15.625 meters at either side of the columns and one weaker 93.75m section at the midspans. This sandwich design more closely models the bridge compared to assuming a constant girder design, at the cost of time spent modelling. Pontoons are large volume floating bodies, but due to their large spacing the hydrodynamic interaction between them is neglected.

Wind loads are neglected despite their relevance to bridge design. For installation analysis there is an option to postpone installation due to high wind speeds. Under normal installation the maximum wind loads can therefore be limited and are expected to be of low significance in modelling. Additionally, due to the limited time available it was decided that hydrodynamic response would be the focus of the thesis.

2.1.1 Wave characteristics

The JONSWAP wave spectrum is used as a representation of the wave conditions in the fjord. JONSWAP is a modified Pierson-Moskowitz spectrum that improves on the original model by increasing the peak values to more accurately match measurements made in the North Sea, figure 7 (Hasselmann et al., 1973). The spectrum is Gaussian and accurately model the generally short, crested waves present in the fjord (Statens Vegvesen, 2018b).

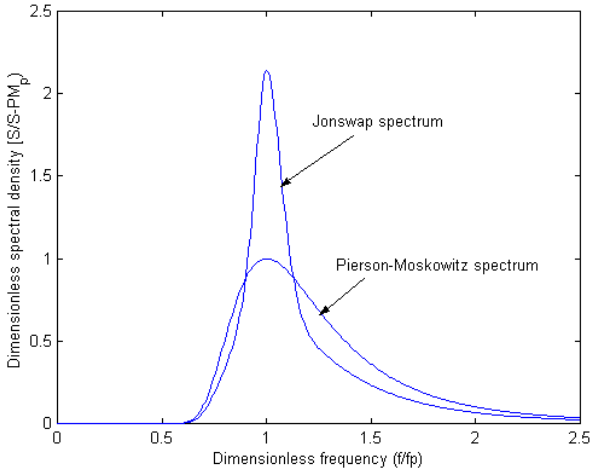

Figure 7: The Pierson-Moskowitz spectrum and the standard JONSWAP spectrum (NTNU, n.d.)

Wave directions are defined by the direction they move relative to the length of the bridge (figure 8). Perpendicular waves have a 90-degree direction of motion while parallel waves move along the length of the bridge girder.

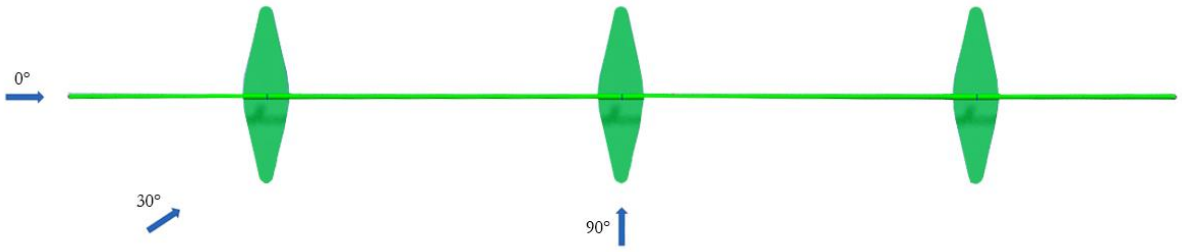

Figure 8: Wave headings

2.1.2 Structural damping

Rayleigh damping is used due to the relevancy of both mass and stiffness-based damping. To find the two proportional damping coefficients the first two eigenvalue frequencies are used in combination with a set damping ratio of 0.5%. α is the stiffness coefficient and β is the mass coefficient. ω_i and ω_j are the first and second natural periods of the structure in Rad/second. ξ_i and ξ_j are both set to 0.005 in accordance to the design basis chapter 8.13.1 (Statens Vegvesen, 2018a).

Natural period 1: 0.2016 Hz = 1.26669 Rad/sec
Natural period 2: 0.2881 Hz = 1.81019 Rad/sec

$$\alpha = \frac{2\,\omega_i\omega_j}{\omega_j^2 - \omega_i^2}\left(\omega_j\xi_i - \omega_i\xi_j\right)$$

$$\beta = \frac{2}{\omega_j^2 - \omega_i^2}\left(\omega_j\xi_i - \omega_i\xi_j\right)$$

The resulting coefficients are:
Mass proportional damping = 0.007448406
Stiffness proportional damping = 0.003251698

2.2 Numerical modelling

This study employs the Sesam DNV package for numerical modelling and analysis. Sesam DNV is a suite of structural engineering software's developed by DNV, all focused on offshore designs and maritime structures. Sesam offers a great advantage by enabling users to go through the entire design process within one single suite of software. One can progress from designing a model to conducting complex loading structural analyses, such as linear and nonlinear static and dynamic analysis, as well as FEM analysis (DNV, 2023d).

Among the suite of software, GeniE, HydroD and Sima are used to obtain necessary results for analysis and further discussion, as illustrated in figure 9 below. The following subsections will provide a brief description of these softwares and how they were utilized.

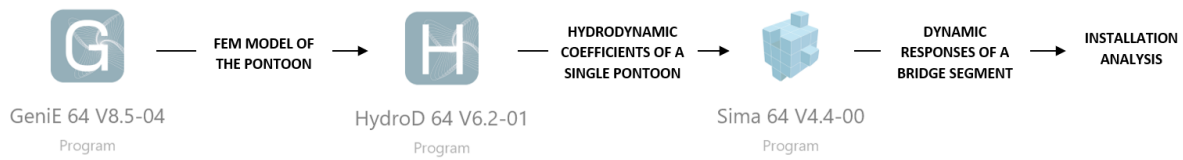

Figure 9: Overview of methodology

2.2.1 GeniE

GeniE is one of the modules of Sesam that provides users with the tools to create finite element models of their structures, from simple box section to a complex 3D geometry (DNV, 2023a). Addition to the geometry, the software allows the user to determine material and thickness of structure, section properties, boundary conditions and loading conditions such as wave loads (DNV - Digital Solutions, 2014). The model can then be used to perform static and dynamic analysis, to further calculate stresses and strains, identify potential weak points and to evaluate the overall structural integrity.

In this study, GeniE is utilized in the first step for the 3D visualization of the pontoon, which is then imported in HydroD in order to further define the necessary parameters and carry out a Wadam-analysis.

After a preliminary modelling using AutoCAD, the pontoon is modelled in GeniE using the specifications provided by Statens Vegvesen. The pontoon cross-section is modelled using four

circles and connected with lines that tangent two adjacent circles. For a quality check, the GeniE model is compared to the AutoCAD model, more specifically at the transition from curvature to linear lines. The 2D model is then duplicated and transposed by the draft, -5 m below the main guideplane representing the free water surface (figure 10).

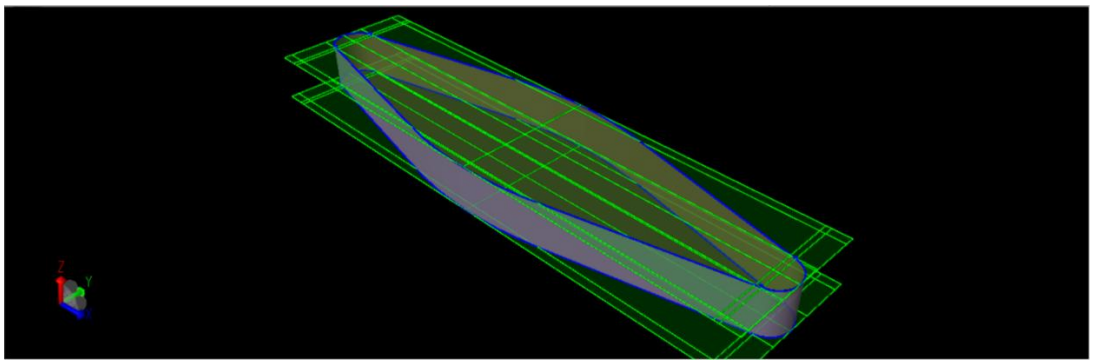

Figure 10: Guideplanes, lines and plates visualization from GeniE

Using the plate tool, the walls of the pontoon are added before designating the outer draft walls as "*Wet surfaces*". A dummy hydro pressure is created and added as a load case on the wet surfaces. As the final step, a mesh is generated with an element length of 1 meter and the wet surfaces are added as a subset. Note that the mesh size is deemed sufficient considering the geometry of the pontoon and the environmental wave conditions. The result is a FEM model with arrows pointing in the direction of the hydrostatic pressure on the pontoon (figure 11).

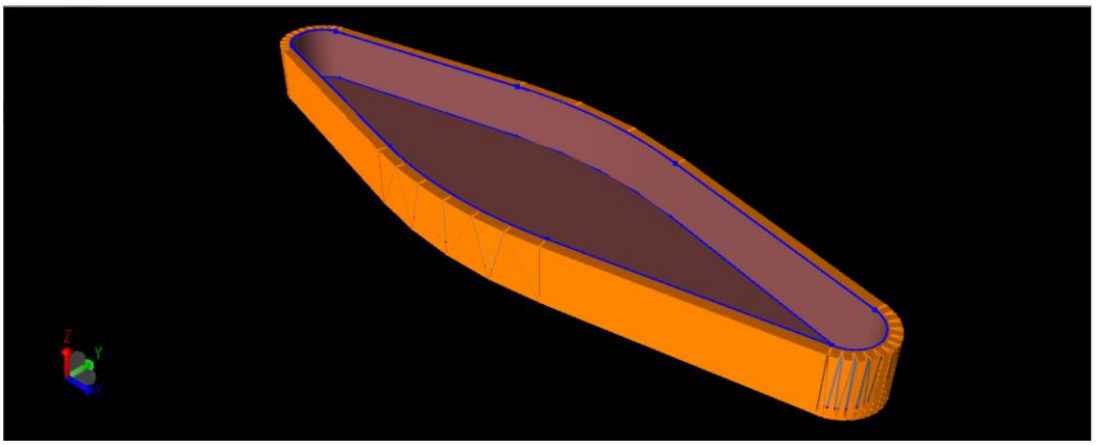

Figure 11: Final geometry in GeniE

2.2.2 HydroD

The second step of the process of extracting results involves performing a hydrodynamic analysis to evaluate the hydrodynamic coefficients including the added mass, potential damping and excitation forces in the frequency domain. HydroD is the go-to software for analyzing any type of floating structure, offering of both stability analysis, frequency and time domain analysis, all based on a single model (DNV, 2023b).

Since it is necessary to understand the performance and safety of the pontoon in open water, only a hydrodynamic analysis is conducted to provide a solution to the issue statement based on relevant results; hydrostatic analysis is omitted. A hydrodynamic analysis is used to study the dynamics of an object, such as its buoyancy, resistance, and flow forces, yielding more beneficial outputs.

HydroD will compute hydrodynamic coefficients using the Wadam analysis, which are numerical values that represent the forces acting on the pontoon in response to its movement through the water. These coefficients are used to simulate the effect of the water on the pontoons motion and will be necessary in further work in Sima for the seakeeping analysis in the time domain.

To proceed with a HydroD Wadam analysis, the environment of the analysis needs to be specified. This will also set a framework, in terms of which directions and sequences extraction of results are desirable. Considering the symmetry of the geometry, the wave headings are taken for directions from 0 to 90 degrees, 15 degrees per step, with frequency from 0,5s to 10s, 0,1s per step.

Later in the process, the analysis requires adding a hydromodel and associated loading conditions, mass, center of gravity and panel model also referred to as the water surface. The pontoon has a total height of 8.5 meters, of which 5 meters is underwater (Statens Vegvesen, 2018a). The illustration below (figure 12) depicts the pontoon, accompanied by arrows indicating hydropressure, and a gray ball representing the object's mass and the location of its center of gravity.

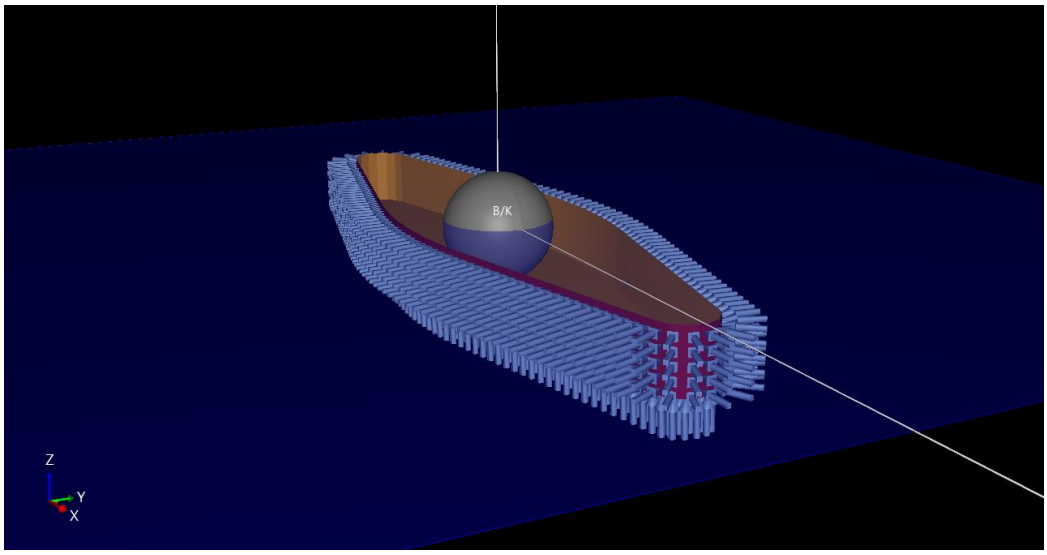

Figure 12: Pontoon visualization in HydroD

2.2.3 Sima

Sima, as the final step, is a powerful marine operations and mooring analysis software designed to help users determine the best strategy for floating structures in a variety of conditions. Sima takes into account the combines effects of wind, current, and waves, and provides efficient calculations for complex, multi-body systems utilizing two core solvers, SIMO and RIFLEX (DNV, 2023c). SIMO is a time domain solution for floating structures and offshore installation, which utilizes frequency-dependent inputs from HydroD (Wadam) to perform time domain analysis. SIMO covers elements such as springs and wires. RIFLEX is a time domain solver that can accommodate flexible elements such as beams and bars through a combination of SIMO rigid body (time domain solver) and finite element formulation.

Previously, a simplified hydrodynamic analysis of a single pontoon has been conducted. Subsequently with Sima, the primary objective is to obtain results for a full bridge segment and analyze its motion response, as well as to calculate maximum and minimum values, mean and standard deviations of the segment. This involves visualizing a bridge segment with variable of pontoons, along with columns and a bridge girder, and input necessary parameters. The work will be carried out in RIFLEX, as this solver also includes SIMO; SIMO will cover the pontoons, while RIFLEX will cover the columns and the bridge girder.

To begin creating a bridge segment in Sima utilizing RIFLEX, the first step is to create supernodes at different coordinates, with constraint and boundary conditions. The supernodes serve as connection points for the connection of the bridge flexural components. When inserting

pontoons (defined as bodies in Sima), they will be connected to a node with the corresponding coordinates. Similarly, columns and the bridge deck (defined as lines in Sima) will also be connected to these supernodes.

Each body (i.e. pontoon) has a kinetic and specified force folder where the values such as the pontoon's weight and buoyancy have been modified, as well as mooring stiffness at each end of the bridge segment in the x and y direction. The modifications in HydroD are done to compensate for the missing superstructure in the initial model. When modelling the pontoon itself, the set draft depth will not produce an equilibrium with the mass of the pontoon in relation to the displaced water. If the mass of the pontoon was defined as the real mass of the steel, the pontoon would float with a much shallower draft. To compensate for the eventual superstructure the initial pontoon model has mass that also includes the columns and girder above. When modelling the superstructure in Sima, the mass of the pontoon is set to its correct value.

RIFLEX also includes an environment folder which must be configured to run the analysis. The analysis utilizes the JONSWAP spectrum for irregular wave analyses and considers waves with different parameters including the significant wave height, peak period and wave heading. Due to the time constraint, the effect of wind and current is neglected in this study. This may be reasonably argued by the fact that the bridge segment installation should be conducted under calm water conditions where the wind and current speeds are expected to be small enough.

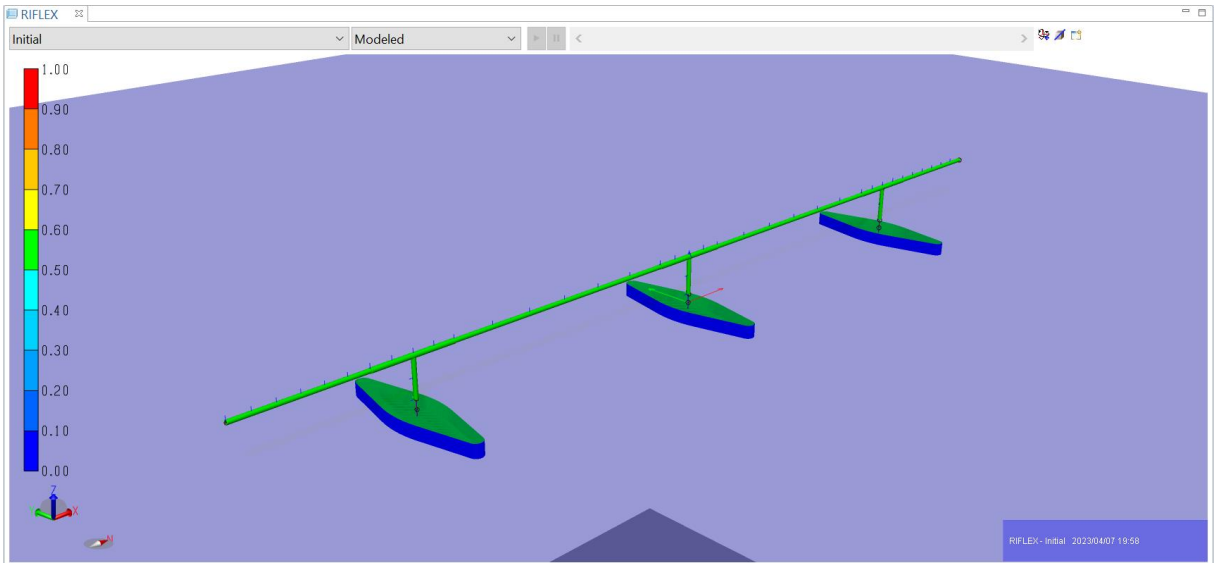

Figure 13: The bridge segment in Sima

The bridge segment is composed of 375 meters of bridge girder constructed with three pontoons. Each pontoon is placed 125 meters apart and the segment ends with a girder of 62,5 meters on either side (figure 13).

3 Presentation of the analysis

The data presented in chapter 3 are based on simulations performed using Sima. As outlined in chapter "*2.2.2 HydroD"*, the underpinning of Sima simulations is based on the results of HydroD. Frequency-dependent hydrodynamic coefficients such as added mass, potential damping and response variables for a single pontoon are used in Sima for the time domain analysis of a bridge segment and are presented in figure 14-16. In figure 14, from left to right, the graph displays the added mass, potential damping, and excitation force along surge-axis. While figure 15 shows the same data correspondingly for sway-axis and figure 16 for heave axis.

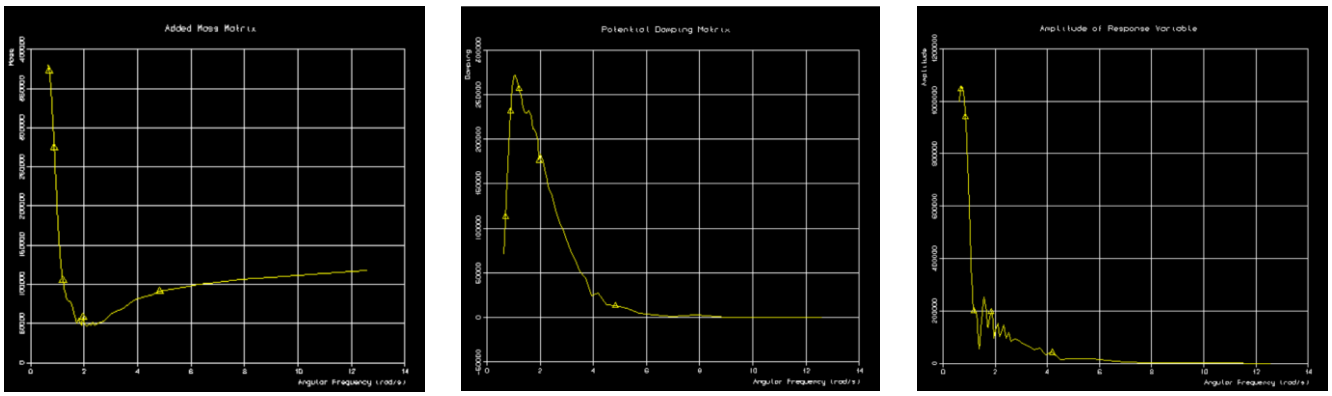

Figure 14: Added mass, potential damping and excitation force along surge-axis

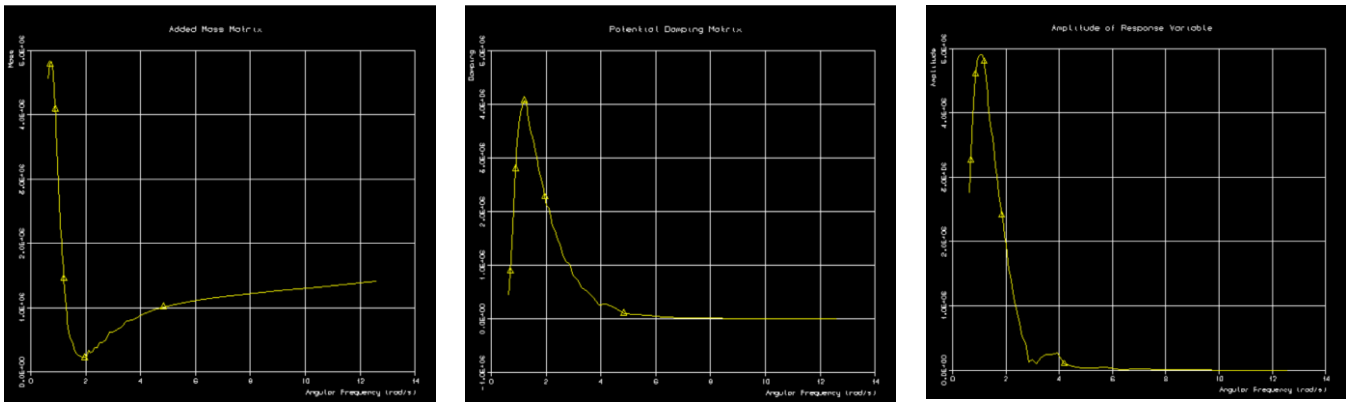

Figure 15: Added mass, potential damping and excitation force along sway-axis

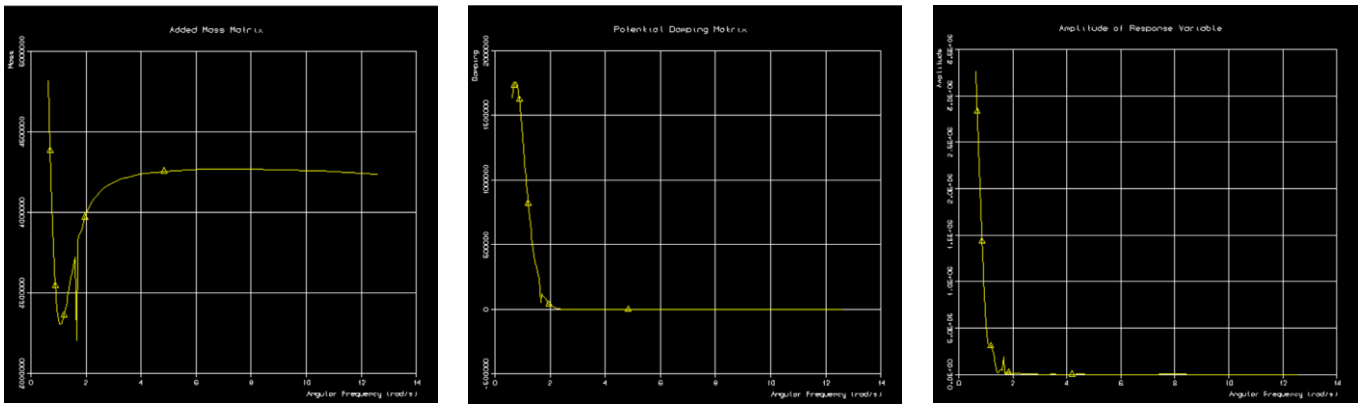

Figure 16: Added mass, potential damping and excitation force along heave-axis

The bridge segment is analyzed in Sima in a JONSWAP wave spectrum with a unidirectional spreading type, 11 directions, a significant wave height of 0.2, a peak period of 4.0, and a gamma of 3.3 (table 3). These values are determined through all dynamic analyses, but the wave direction will vary. Section 3.1 presents and discusses wave direction 90 degrees. Section 3.2 investigates how the bridge segment responds in bending moment about y- and z-axis, by increasing the wave height. In final section 3.3, the bridge segment is examined and compared in three different wave conditions with wave directions of 90-, 30- and 0-degrees (figure 8). The analysis will allow an understanding of how the bridge segment responds to different wave height and directions and form the basis to continue with an evaluation of which wave condition is best suited for installation. Table 3 provides data detailing the different wave conditions evaluated.

Table 3: Wave conditions

Direction (Degrees)	Spreading Type	Number of Directions	Significant Wave Height (meters)	Peak Period (seconds)	Gamma
90	Unidirectional	11	0.2 0.35 0.5	4.0	3.3
30	Unidirectional	11	0.2	4.0	3.3
0	Unidirectional	11	0.2	4.0	3.3

Nedrebø's presentation establishes a criterion of 0.5-meter for the assessment of wave heights (Nedrebø, 2016). Subsequently, new values were defined to identify the magnitude of the wave heights influence.

Due to the complexities of visualizing dynamic responses in a structure over time, absolute maximum values are combined across a specific time duration considered in this study. In this study, the total simulation length is set to 3600 seconds. As the initial phases contain transient responses due to e.g., the sudden application of environmental loads, the first 600 seconds of results are discarded. Absolute maximum values created more intuitive results, as two values next to each other could be either negative or positive. In combination with line graphs or scatter plots this led to lines crossing the x-axis or points that were hard to visualize as a trend. Besides, in the design practice the absolute maximum values are needed to check the design adequacy of the structural components.

3.1 Reaction forces with 90 degrees in wave propagation direction

Presented in 3.1 are results from simulation performed through Sima, where the bridge segment is exposed to 90 degrees wave direction and 0.2-meter wave height. The presentation will include reflection of reaction forces, such as bending moments and shear forces, in both the y- and z-direction, as well as torsion.

3.1.1 Moment about y- and z axis

The bending moment around the y- and z-axis along the bridge girder is generated as a result of hydrodynamic forces which seek to cause a rotation around the axis of the bridge girder. The rotations are typically referred to as "pitch" for rotation around the y-axis and "yaw" for rotation around the z-axis. Pitch occurs when the pontoon bridge is exposed to horizontal forces, causing it to dip up and down consequently creating a bending moment. Yaw, on the other hand, is when the bridge girder experiences vertical forces, causing it to turn on its axis, which in turn generates a twisting force.

In perpendicular wave conditions the results (Figure 17) show compliance with expected maximum values. Graphs are plotted with the maximum absolute values across the length of the bridge. For 90-degree waves the maximum bending moments occur at the outsides of external pontoons, with peaks at maximum 1307.3 MNm. For hogging moments, the peaks are located at the insides of external pontoons with -894 MNm maximum values. Moment graphs show good symmetry; however, the right side does trend slightly lower than the left side. This may be due to modelling and analysis uncertainties, however due to the complexity of visualizing dynamic

analysis it is difficult to pinpoint the origin. The general shape and trend of graphs presented all fall within the expected range.

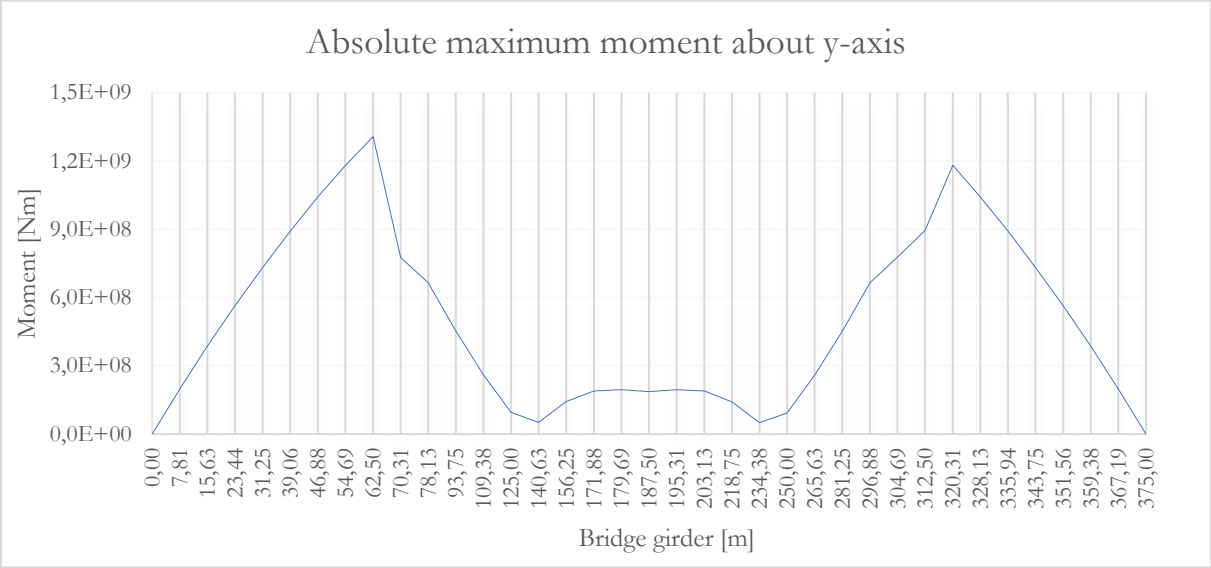

Figure 17: Absolute max moment about y-axis, 90 degrees in wave propagation direction

Horizontal moments show good symmetry with a maximum value at the bridge midpoint (Figure 18). This is expected due to the mooring design, as the bridge is only transversely supported at either end pontoon the midpoint will naturally have the highest values for horizontal bending. The results for strong-axis bending are 2 orders of magnitude smaller than the weak axis bending presented above. Moment values about the z-axis are also well within the expected range, as the model is of a truncated bridge section without wind loading the horizontal forces are much lower than the bridge capacity.

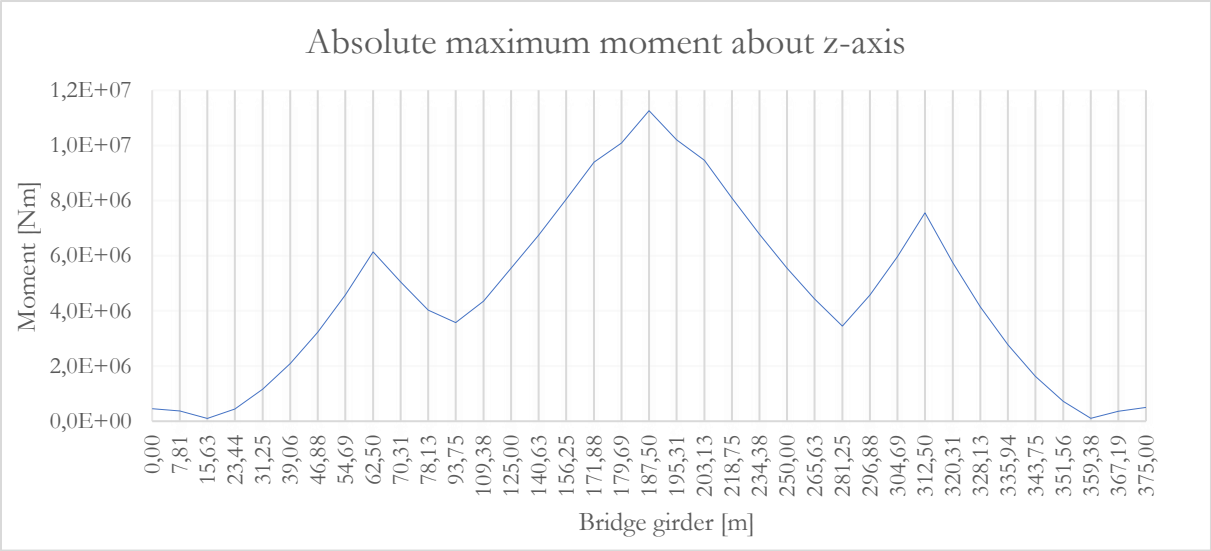

Figure 18: Absolute max moment about z-axis, 90 degrees in wave propagation direction

3.1.2 Torsion moment

Torsion moment forces occur along a bridge girder when external forces cause the bridge girder to twist or rotate about the longitudinal axis. Torsion applied to a bridge girder causes it to deform in cross-section shape, as well as in its overall shape. These deformations can potentially cause bridge failure, so it is crucial to appropriately account for torsion moment forces when designing and constructing bridge girders.

Torsion results are exported from Sima on either end of each element, before being combined into one graph. As Sima calculates torsion as constant throughout each element, two bordering elements will have equal torsion values on connecting faces.

Absolute maximum torsional moments are relatively symmetrical (Figure 19) and show a baseline for later comparison. During assembly large barges support the ends of the bridge to stabilize during transport. These barges will create additional torsional restraint in addition to vertical support.

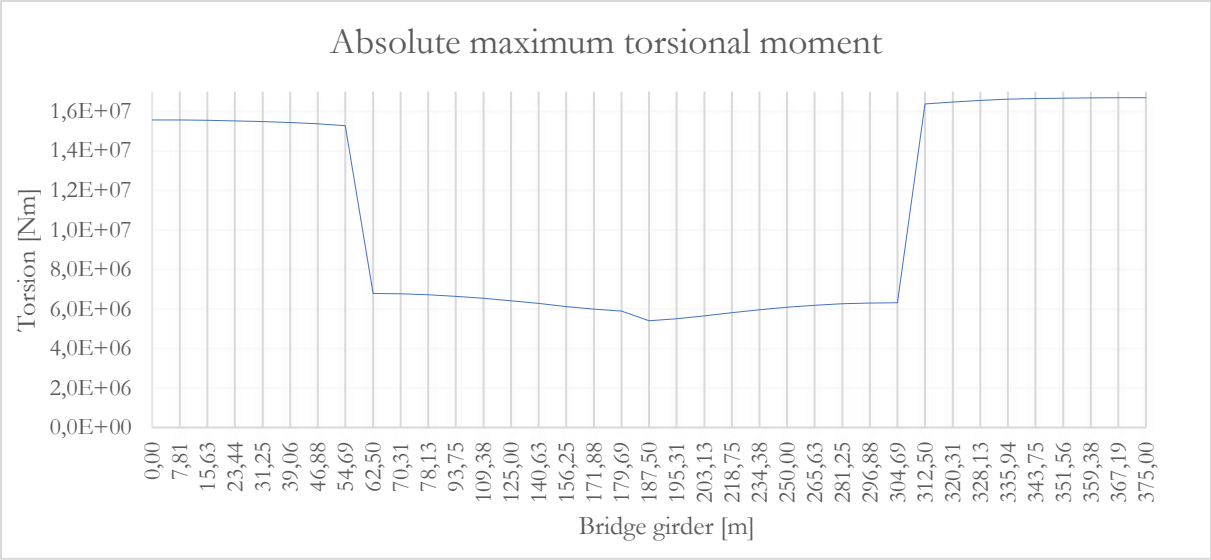

Figure 19: Absolute max torsional moment along the bridge girder, 90 degrees in wave propagation direction

3.1.3 Shear force in y- and z- direction

The horizontal shear force shows a three-peak graph with peaks between 188840 N on the first pontoon and 218780 N on the third pontoon (figure 20). Peak values occur at pontoon locations where large changes in shear are expected. Midspans between pontoons have the lowest values at 79.3 kN at 140m and 84.3 kN at 250m.

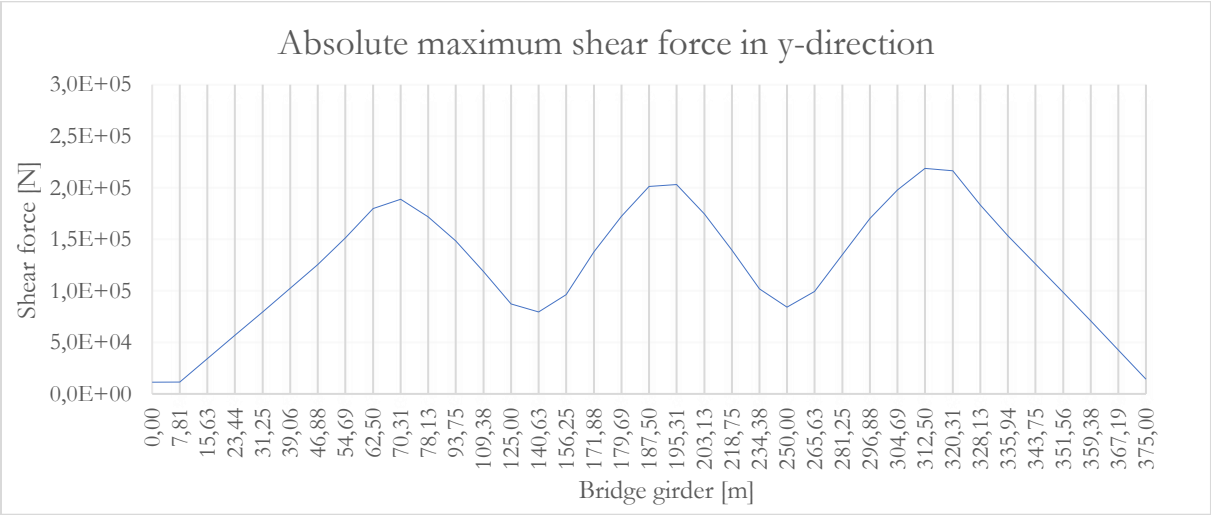

Figure 20: Absolute max shear force in y-direction, 90 degrees in wave propagation direction

Vertical shear with 90 degree waves follow a V-shape with peaks at either end (figure 21). Due to the supporting barges modelled as fixed supports, the vertical shear at both ends also includes the reactions due to wave-induced dynamic forces thus the outermost points of the graph do not equal zero.

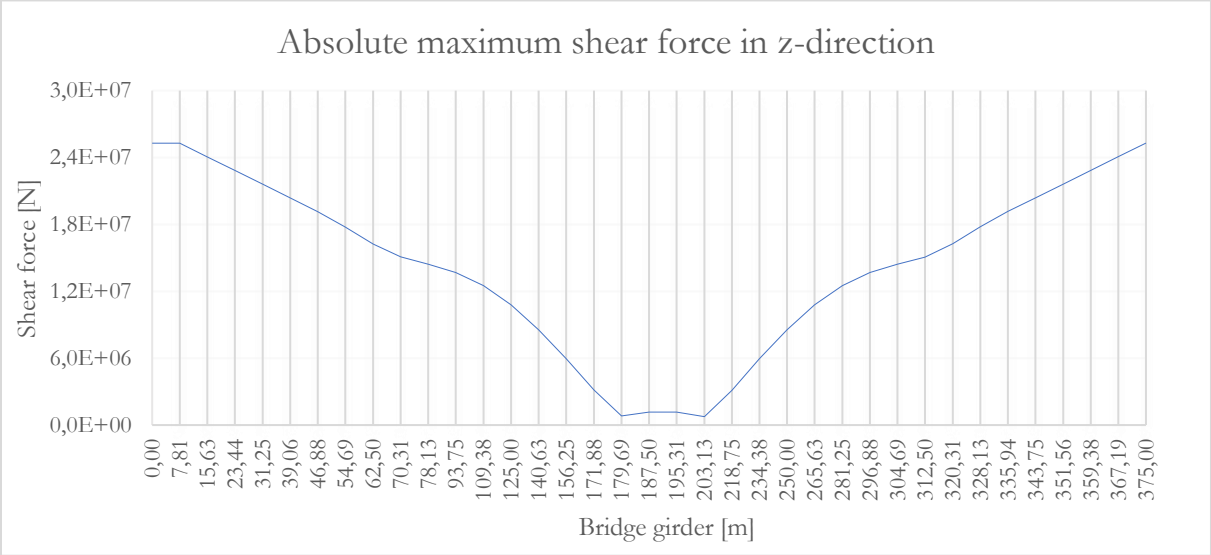

Figure 21: Absolute max shear force in z-direction, 90 degrees in wave propagation direction

3.2 Effect of increasing wave height

Allowing for larger wave heights during assembly can increase the distance it is possible to transport bridge sections by widening the window for assembly. How much increased wave heights impact the response in the bridge structure is dependent on multiple factors such as the wave spectrum, structural damping, support conditions and more. Moments about the y-axis have peak values at the external pontoons (62,5 m) shown in figure 17. Moments around the z-axis peak at the midpoint of the bridge (187,5 m) shown in figure 18.

Wave heights are plotted against their subsequent maximum moments. Results show that vertical bending moments are linearly related to the wave heights (Figure 22). This is expected as the vertical motions will increase under increased wave heights. The linear increase is small, with a <1% increase from 0.2-0.5 m waves. Horizontal moments are however not linearly related, with one possible source being wave drift. As wave heights increase the horizontal forces acting on the structure also increases. If horizontal forces are large enough that the mooring lines do not restore the bridge to its original location before the next wave, the structure will start drifting with the waves. As mentioned earlier in the chapter, horizontal moments are significantly lower compared to the full bridge model due to the lack of wind forces and the shorter bridge length. It is therefore not as problematic that the relation between wave height and horizontal moments are not linear. It does however show that wave height could negatively impact assembly as the 150% increase in height from 0.2m waves to 0.5m multiplies the horizontal moments by 200%.

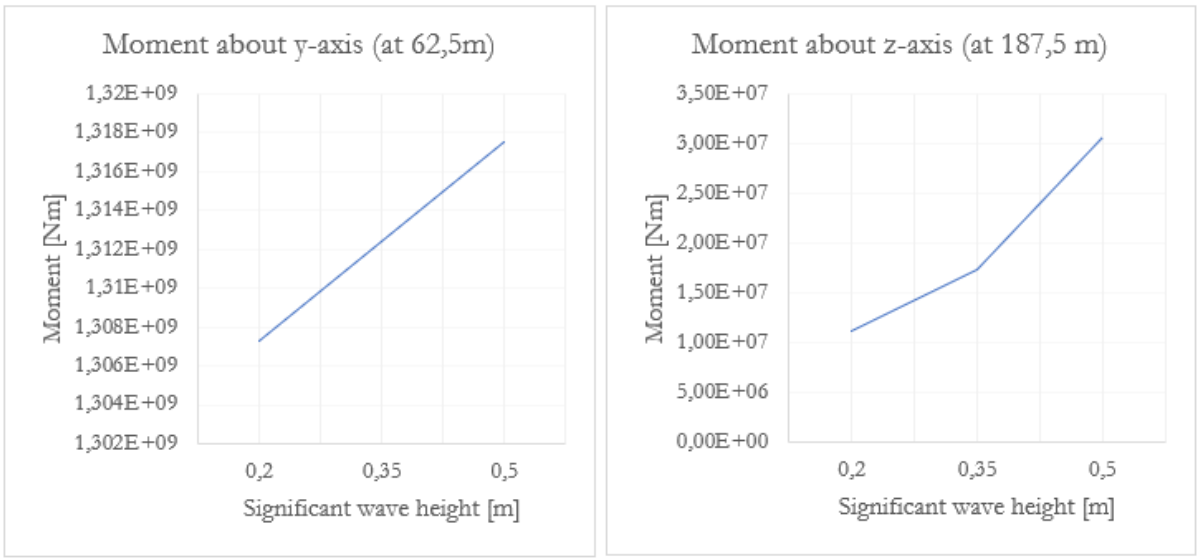

Figure 22: Effect on bending moment about y- and z-axis with increasing wave height

3.3 Comparison between different wave headings

Under construction of large projects there are often allowances for certain environmental conditions. For marine environments the wave height and wind speed are highly relevant variables that could significantly affect the transportation and assembly of large structures. Wave headings are one variable that potentially could lead to changes in the behavior of the bridge. Three wave headings are compared below, perpendicular waves (90-degree) from the previous chapter, sharp waves (30-degree), and parallel waves (0-degree). Wave variables plotted in JONSWAP are presented in table 3 with significant wave height equal to 0.2 in all three cases.

3.3.1 Moment about y- and z-axis

Vertical bending moments remain consistent independently of the wave headings (figure. 23). This is expected as wave height is the main contributor to vertical motion. It is however important to note that while maximum values are virtually unaffected, despite the change in the wave heading.

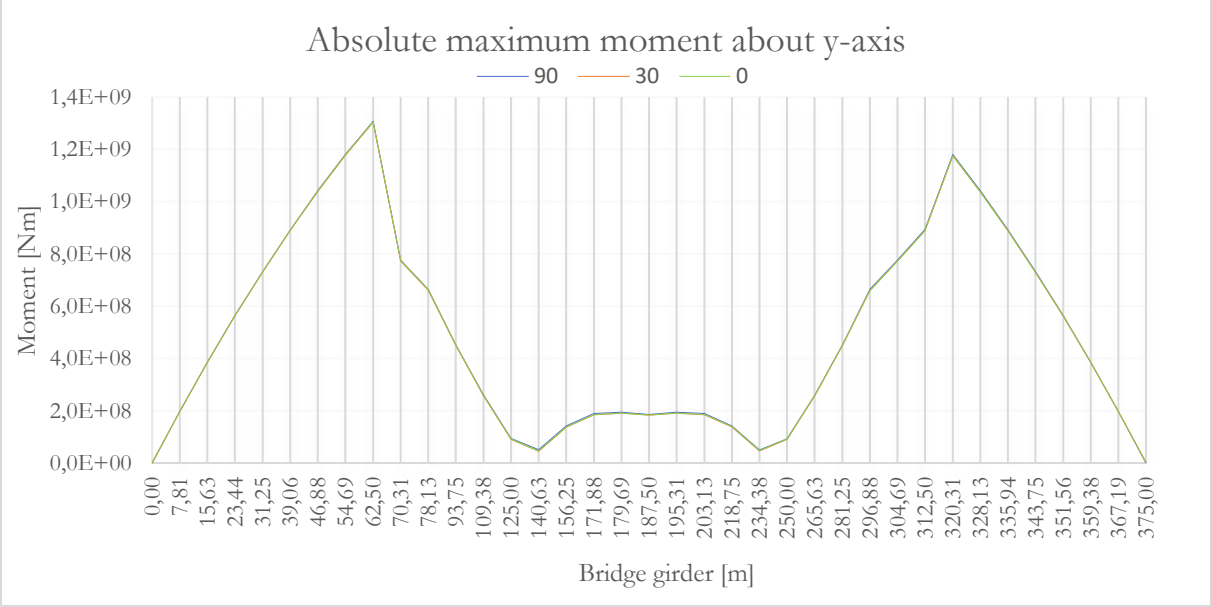

Figure 23: Comparison of absolute max moment about y-axis with different wave headings

Absolute maximum moments around the z-axis results (Figure 24) show peak values at pontoon locations. This is expected as the middle pontoon is not moored, and therefore falls at the midpoint between the two restrained pontoons. As this is a dynamic analysis the outside of

external pontoons still has moments around the z axis. The horizontal vibrations of the bridge girder will create forces and moments even though there is no horizontal restraint there.

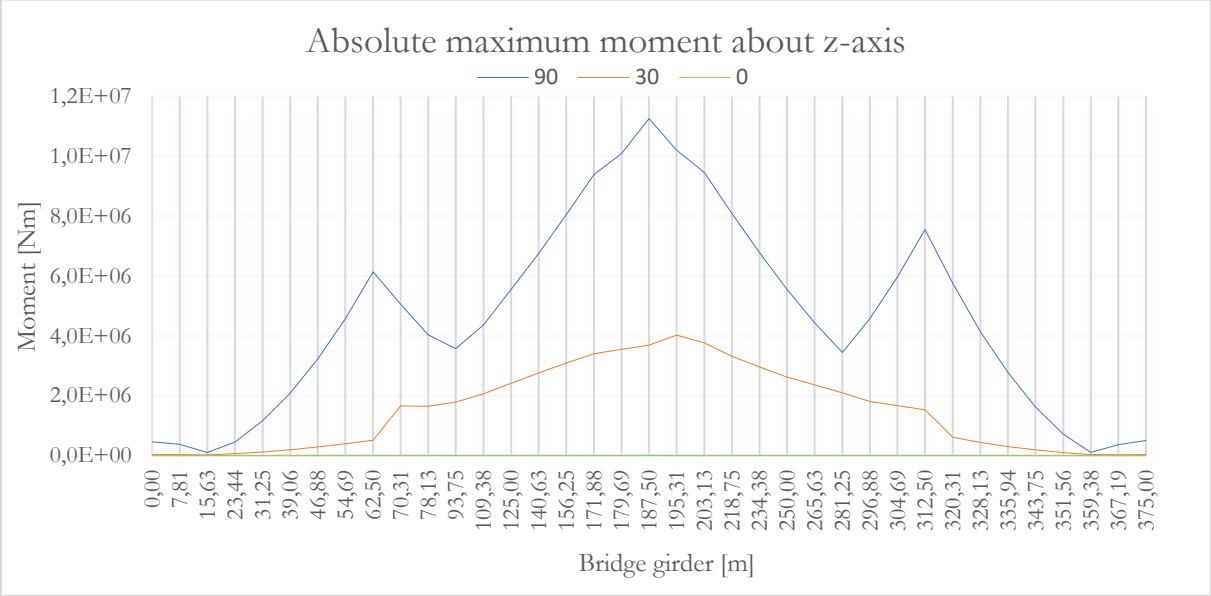

Figure 24: Comparison of absolute max moment about z-axis with different wave headings

3.3.2 Torsional moment

Torsional moments are higher under perpendicular wave conditions especially on the girder outside of the external pontoons (Fig. 25). Torsional moments for parallel waves are close to zero with a 576.74 Nm peak at 0 meters.

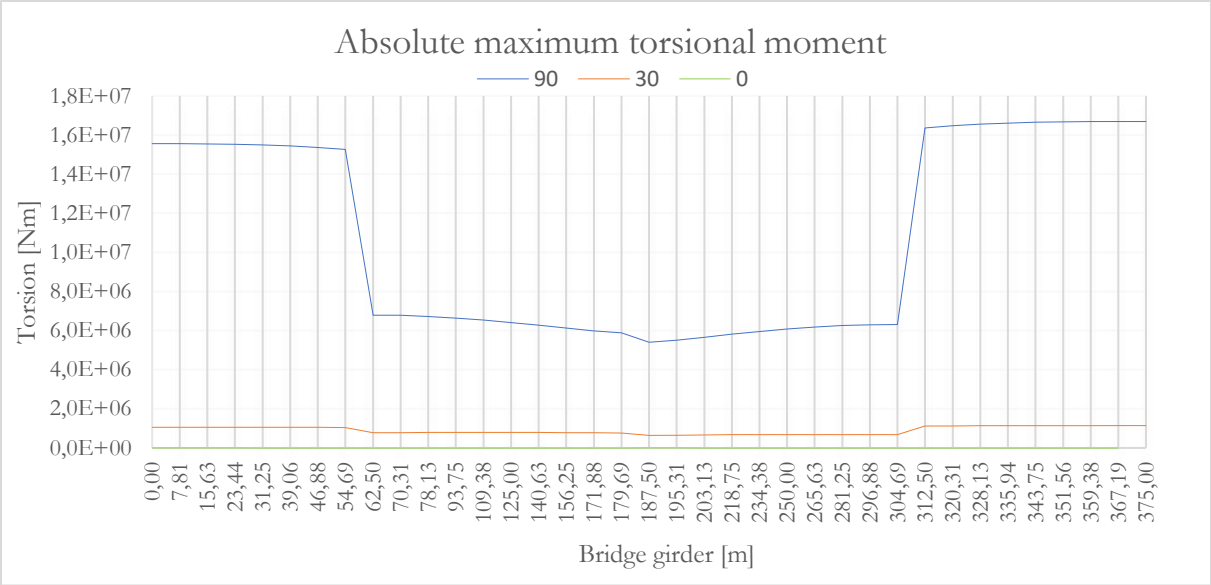

Figure 25: Comparison of absolute max torsional moment with different wave headings

3.3.3 Shear force in y- and z-direction

The horizontal shear force, figure 26, shows little change compared to the non-parallel directions. The parallel waves do not induce any perpendicular shear, which is also expected. Vertical shear force (z-direction) is largely unaffected by the wave direction, see figure 27.

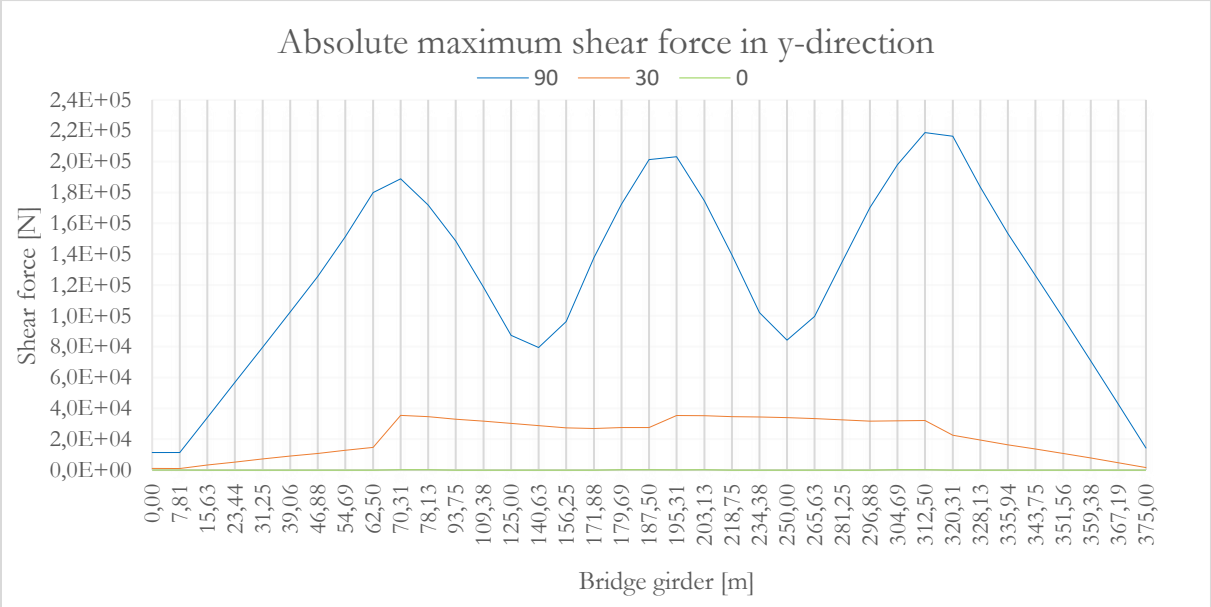

Figure 26: Comparison of absolute max shear force in y-direction with different wave headings

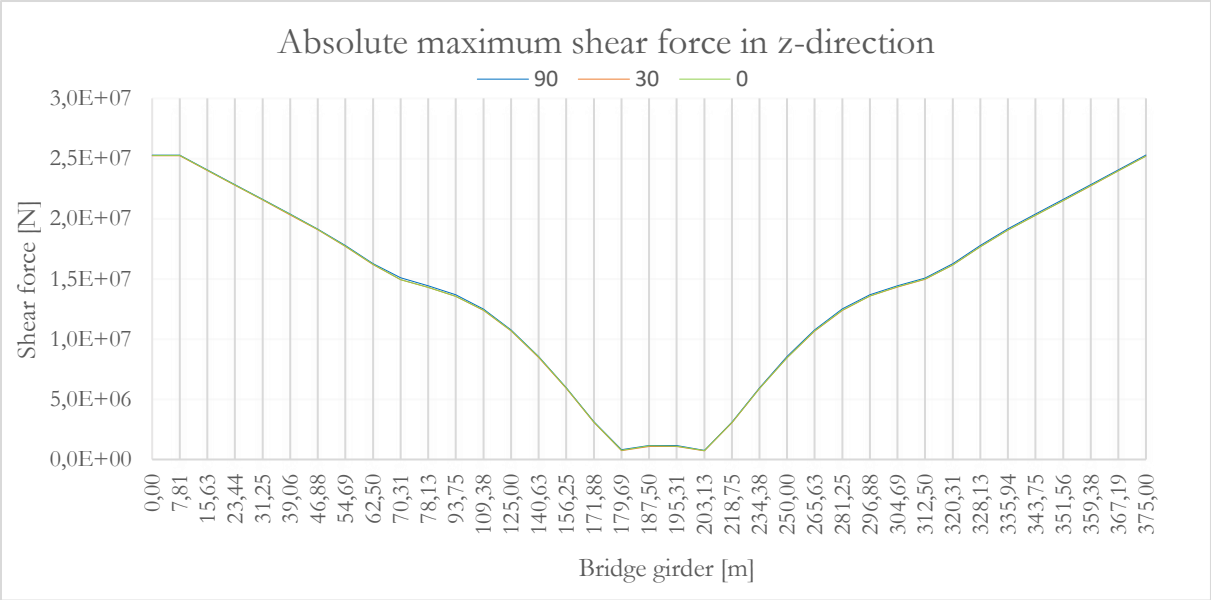

Figure 27: Comparison of absolute max shear force in z-direction with different wave headings

4 Conclusions and future work

In this thesis a truncated floating bridge section was modelled according to the Bjørnafjorden floating bridge design proposed by Multiconsult. The 375m bridge section consists of three pontoons with bridge girders between them and half of the external bridge spans. Both external pontoons are moored to limit horizontal motion but are free to rotate and heave. During assembly the free hanging bridge ends are supported using barges to add rotational stiffness. Mooring lines are modeled as springs while barges are modeled as rigid supports.

A numerical study has been conducted to compare the effects of three wave headings (90, 30, 0 degrees) and three wave heights (0.2, 0.35, 0.5). Waves are modeled using a JONSWAP spectrum in accordance with the design basis. Findings show that the truncated floating bridge model is more subject to changes in wave directions during assembly compared to wave heights. Perpendicular wave directions induce more moments in the bridge girder, compared to parallel waves. When increasing the wave height from 0,2 to 0,35 and then 0,5 meters there is <1% change in peak moments about the horizontal axis. However, the moments about the vertical axis increase by 200%. This may be because weak axis bending is dominated by the self-weight of the bridge girder for the wave conditions considered in this study. The effect of wave heights on the strong axis bending is more dominating, however the values are low compared to the structural capacity.

Limitations

This study does not consider the wind loads despite often being the dominant horizontal forces on floating structures. When installing large floating structures limitations for allowed wind speeds and wave heights are set. Isolating wave heights and wave direction focuses on the bridge girders weak vertical axis. Horizontal loads on a truncated bridge section will be significantly lower compared to the completed bridge. This is in part due to the much shorter distance between mooring clusters, but also because maximum wind speeds are based on extreme weather events that would postpone the installation in practice.

Future work

Both free ends of the model are supported by fixed points that represent barges used during installation. As these barges will act as floating bodies with their own mass, geometry and hydrodynamic response, it would be beneficial in the future to model these barges in equal detail to the bridge section.

Wave peak heights and wave directions are two of the factors that determine the wave conditions. For future work a numerical study comparing wave peak periods could further develop the understanding of wave characteristics on truncated bridge sections. Adding more wave heights and directions in different combinations would also be beneficial as there might be combinations of these factors that induce more moments in the bridge girder.

There are several design checks for driving comfort in a completed bridge. It is equally important to consider worker comfort and safety during assembly. Detailing the vertical and horizontal acceleration and motion could determine what work can be done optimally during different conditions, and whether postponements are necessary.

5 Reference list

Cui, M., Cheng, Z., & Moan, T. (2023). Effects of inhomogeneous wave modeling on extreme responses of a very long floating bridge. *Applied Ocean Research*, *134*, 103505. https://doi.org/10.1016/j.apor.2023.103505

Dai, J., Abrahamsen, B. C., Viuff, T., & Leira, B. J. (2022). Effect of wave-current interaction on a long fjord-crossing floating pontoon bridge. *Engineering Structures*, *266*, 114549. https://doi.org/10.1016/j.engstruct.2022.114549

Dai, J., Leira, B. J., Moan, T., & Kvittem, M. I. (2020). Inhomogeneous wave load effects on a long, straight and side-anchored floating pontoon bridge. *Marine Structures*, *72*, 102763. https://doi.org/10.1016/j.marstruc.2020.102763

DNV. (2023a). *Conceptual modelling of offshore and maritime structures | GeniE*. DNV. https://www.dnv.com/services/conceptual-modelling-of-offshore-and-maritime-structures-genie-89128

DNV. (2023b). *Hydrodynamic analysis and stability analysis software | HydroD*. DNV. https://www.dnv.com/services/hydrodynamic-analysis-and-stability-analysis-software-hydrod-14492

DNV. (2023c). *Marine operations and mooring analysis software | Sima*. DNV. https://www.dnv.com/services/marine-operations-and-mooring-analysis-software-sima-2324

DNV. (2023d). *Sesam Portal*. https://sesam.dnv.com/

DNV - Digital Solutions (Director). (2014, August 5). *Sesam GeniE: Beginner Tutorial*. https://www.youtube.com/watch?v=yZAwbq1hRh8

Douglas, C. R. (2013, August 27). *520 Bridge pontoon problems could reach nearly $400 million | Q13 FOX News*. https://web.archive.org/web/20160605114811/http://q13fox.com/2013/08/27/520-bridge-pontoon-problems-could-reach-nearly-400-million/

Hasselmann, K., Barnett, T. P., Bouws, E., Carlson, H., Cartwright, D. E., Eake, K., Euring, J. A., Gicnapp, A., Hasselmann, D. E., Kruseman, P., Meerburg, A., Mullen, P., Olbers, D. J., Richren, K., Sell, W., & Walden, H. (1973). *Measurements of wind-wave growth and swell decay during the joint North Sea wave project (JONSWAP)*. https://www.scopus.com/inward/record.uri?eid=2-s2.0-0015559626&partnerID=40&md5=82cd454eff78dc7906e775a3642cb922

Hove, K. J., Hasselø, J. A., & Johnsen, H. I. (2015, September 22). *Costal Highway Route E39 Project*. https://www.vegvesen.no/globalassets/vegprosjekter/utbygging/ferjefrie39/vedlegg/12-and-13-coastal-highway-route-e39strategies-and-contract-types-kjartan-hove-and-harald-inge-johnsen.pdf

Maruyama, T., & Kawamura, Y. (2000). *Construction of a Floating Swing Bridge—Yumemai Bridge*.

Moe, S. (1995). *The Nordhordland Bridge: Europe's longest floating bridge crosses the Salhus Fjord 1995*. Statens vegvesen, Hordaland.

Nedrebø, Ø. (2016, September 20). *Floating bridge E39 Bjørnafjorden*.

Norconsult. (2019). *K12 – Summary report*. https://vegvesen.brage.unit.no/vegvesen-xmlui/bitstream/handle/11250/2660421/SBJ-33-C5-OON-22-RE-100-0%20K12%20-%20Summary%20report_sladdet.pdf?sequence=1&isAllowed=y

NTNU. (n.d.). *3 SEA STATE PARAMETERS AND ENGINEERING WAVE SPECTRA*. https://folk.ntnu.no/oivarn/hercules_ntnu/LWTcourse/partB/3seastate/3%20SEA%20STATE%20PARAMETERS%20AND%20ENGINEERING%20WAVE%20SPECTRA.htm

Sha, Y., Amdahl, J., & Dørum, C. (2017). Dynamic responses of a floating bridge subjected to ship collision load on bridge girders. *Procedia Engineering*, *199*, 2506–2513. https://doi.org/10.1016/j.proeng.2017.09.425

Statens Vegvesen. (2017). *Bjørnafjorden, straight floating bridge phase 3 Analysis and design (Base Case)*. https://www.vegvesen.no/globalassets/vegprosjekter/utbygging/e39stordos/vedlegg/sbj-31-c3-mul-22-re-100-0-analysis-and-design-base-case.pdf

Statens Vegvesen. (2018a). *Design Basis Bjørnafjorden floating bridges*. https://vegvesen.brage.unit.no/vegvesen-xmlui/bitstream/handle/11250/2676915/SBJ-32-C4-SVV-90-BA-001%20-%20Design%20Basis%20Bj%C3%B8rnajorden%20Rev%200.pdf?sequence=4&isAllowed=y

Statens Vegvesen. (2018b). *MetOcean Design basis*.

Wang, C. M., & Tay, Z. Y. (2007). *Very Large Floating Structures*.

Watanabe, E., Maruyama, T., Tanaka, H., & Takeda, S. (2000). Design and construction of a floating swing bridge in Osaka. *Marine Structures*, *13*(4), 437–458. https://doi.org/10.1016/S0951-8339(00)00016-2

Wikipedia. (2023). Nordhordlandsbrua. In *Wikipedia*. https://no.wikipedia.org/w/index.php?title=Nordhordlandsbrua&oldid=23445856

Wilma, D., & Oldham, K. (2005, August 16). *WSDOT abandons Hood Canal bridge graving dock project located on site of Klallam Indian village and cemetery on December 21, 2004. - HistoryLink.org*. https://www.historylink.org/File/7344

Zhengshun, C., Zhen, G., & Moan, T. (2018, February 6). *Hydrodynamic load modeling and analysis of a floating bridge in homogeneous wave conditions*. https://doi.org/10.1016/j.marstruc.2018.01.007

Appendix

Values presented in the appendix are the results exported from Sima with negative values highlighted in red. The sign indicates the direction of the quantities when the absolute maxima occur.

A1 Moment about y- and z-axis with 90 degrees in wave propagation direction

Y – axis	
Bridge girder [m]	**Moment [Nm]**
0	271,73
7,8125	197560000,00
15,625	385530000,00
23,4375	563920000,00
31,25	732720000,00
39,0625	891920000,00
46,875	1041500000,00
54,6875	1180400000,00
62,5	1307300000,00
70,3125	-776470000,00
78,125	-664730000,00
93,75	-453170000,00
109,375	-260040000,00
125	-94340000,00
140,625	51062000,00
156,25	142180000,00
171,875	189110000,00
179,6875	194280000,00
187,5	185950000,00
195,3125	194290000,00
203,125	188930000,00
218,75	141200000,00
234,375	49229000,00
250	-92218000,00
265,625	-257560000,00
281,25	-451900000,00
296,875	-664630000,00
304,6875	-776720000,00
312,5	-894020000,00
320,3125	1180600000,00
328,125	1041700000,00
335,9375	892110000,00
343,75	732870000,00
351,5625	564030000,00
359,375	385610000,00
367,1875	197600000,00
375	-199,44

Z – axis	
Bridge girder [m]	**Moment [Nm]**
0	456900,00
7,8125	369060,00
15,625	101090,00
23,4375	-443440,00
31,25	1159600,00
39,0625	2088500,00
46,875	3227600,00
54,6875	4569900,00
62,5	6139300,00
70,3125	-5054400,00
78,125	-4031000,00
93,75	3574500,00
109,375	4359400,00
125	5549800,00
140,625	6745400,00
156,25	8043800,00
171,875	9392100,00
179,6875	10090000,00
187,5	11259000,00
195,3125	10203000,00
203,125	9456300,00
218,75	8086300,00
234,375	6778900,00
250	5554200,00
265,625	4435700,00
281,25	3448000,00
296,875	4578800,00
304,6875	5965500,00
312,5	7554500,00
320,3125	5750100,00
328,125	4143600,00
335,9375	2776500,00
343,75	1623800,00
351,5625	715570,00
359,375	-104770,00
367,1875	-357750,00
375	-505600,00

A2 Torsion with 90 degrees in wave propagation direction

Torsion tables show the Girder-Segment-Element divisions. End 1 is the Girder only supported on one side. The two beam elements are the bridge spans between pontoons, and End 2 is the second cantilever girder section only supported on the other side.

Part	Segment	Element	Bridge girder [m]	Torsion [Nm]
End 1	1	1	0	15562000,00
		2	7,8125	15557000,00
		3	15,625	15544000,00
		4	23,4375	15524000,00
		5	31,25	15491000,00
		6	39,0625	15441000,00
	2	7	46,875	15368000,00
		8	54,6875	15273000,00
Beam 1	1	9	62,5	6781800,00
		10	70,3125	6762300,00
	2	11	78,125	6723200,00
		12	93,75	6642500,00
		13	109,375	6536100,00
		14	125	6413000,00
		15	140,625	6276900,00
		16	156,25	6125300,00
	3	17	171,875	5991800,00
		18	179,6875	5889200,00
Beam 2	1	19	187,5	5404100,00
		20	195,3125	5513300,00
	2	21	203,125	5656100,00
		22	218,75	5817200,00
		23	234,375	5957600,00
		24	250	6080700,00
		25	265,625	6186300,00
		26	281,25	6265300,00
	3	27	296,875	6300700,00
		28	304,6875	6316900,00
End 2	1	29	312,5	16370000,00
		30	320,3125	16477000,00
	2	31	328,125	16558000,00
		32	335,9375	16614000,00
		33	343,75	16651000,00
		34	351,5625	16673000,00
		35	359,375	16686000,00
		36	367,1875	16691000,00

A3 Shear forces in y- and z-direction with 90 degrees in wave propagation direction

Y – direction	
Bridge girder [m]	**Shear [N]**
0	-11360,00
7,8125	-11365,00
15,625	-34083,00
23,4375	56848,00
31,25	79664,00
39,0625	102540,00
46,875	125500,00
54,6875	-151250,00
62,5	-179870,00
70,3125	-188840,00
78,125	-171800,00
93,75	-148520,00
109,375	-118540,00
125	-87323,00
140,625	-79364,00
156,25	-96174,00
171,875	137760,00
179,6875	-172400,00
187,5	-201230,00
195,3125	203110,00
203,125	-174540,00
218,75	-139500,00
234,375	101970,00
250	84316,00
265,625	99506,00
281,25	135180,00
296,875	170190,00
304,6875	197910,00
312,5	218780,00
320,3125	216430,00
328,125	183400,00
335,9375	153290,00
343,75	126070,00
351,5625	98577,00
359,375	70780,00
367,1875	42664,00
375	14224,00

Z – direction	
Bridge girder [m]	**Shear [N]**
0	25288000,00
7,8125	25288000,00
15,625	24060000,00
23,4375	22833000,00
31,25	21606000,00
39,0625	20378000,00
46,875	19148000,00
54,6875	17772000,00
62,5	16252000,00
70,3125	15083000,00
78,125	14442000,00
93,75	13684000,00
109,375	12500000,00
125	10769000,00
140,625	8555300,00
156,25	5969600,00
171,875	3137200,00
179,6875	806040,00
187,5	-1168200,00
195,3125	1160800,00
203,125	-753620,00
218,75	-3104800,00
234,375	-5958000,00
250	-8555100,00
265,625	-10771000,00
281,25	-12503000,00
296,875	-13674000,00
304,6875	-14422000,00
312,5	-15056000,00
320,3125	-16258000,00
328,125	-17778000,00
335,9375	-19153000,00
343,75	-20383000,00
351,5625	-21611000,00
359,375	-22838000,00
367,1875	-24065000,00
375	-25293000,00

B1 Moment about y- and z-axis with 30 degrees in wave propagation direction

Y – axis	
Bridge girder [m]	**Moment [Nm]**
0	150,25
7,8125	197120000,00
15,625	384660000,00
23,4375	562600000,00
31,25	730960000,00
39,0625	889710000,00
46,875	1038800000,00
54,6875	1177200000,00
62,5	1303700000,00
70,3125	-767070000,00
78,125	-661460000,00
93,75	-449930000,00
109,375	-256470000,00
125	-89836000,00
140,625	45440000,00
156,25	136610000,00
171,875	-184950000,00
179,6875	189410000,00
187,5	181620000,00
195,3125	189980000,00
203,125	184780000,00
218,75	137750000,00
234,375	46198000,00
250	-90054000,00
265,625	-256040000,00
281,25	-448970000,00
296,875	-660080000,00
304,6875	-771410000,00
312,5	-887690000,00
320,3125	1175300000,00
328,125	1037100000,00
335,9375	888290000,00
343,75	729810000,00
351,5625	561740000,00
359,375	384080000,00
367,1875	196840000,00
375	105,33

Z – axis	
Bridge girder [m]	**Moment [Nm]**
0	31919,00
7,8125	26037,00
15,625	-24741,00
23,4375	-59442,00
31,25	-120020,00
39,0625	-196300,00
46,875	-287670,00
54,6875	-394500,00
62,5	-517110,00
70,3125	-1658000,00
78,125	-1641200,00
93,75	1789000,00
109,375	2067600,00
125	2420600,00
140,625	2762200,00
156,25	3088500,00
171,875	3397000,00
179,6875	3548500,00
187,5	3692900,00
195,3125	4023400,00
203,125	3765600,00
218,75	3312100,00
234,375	2967000,00
250	2620200,00
265,625	2362300,00
281,25	2090500,00
296,875	1808400,00
304,6875	1671700,00
312,5	1531300,00
320,3125	605450,00
328,125	442230,00
335,9375	302810,00
343,75	187710,00
351,5625	97178,00
359,375	-31241,00
367,1875	-23302,00
375	-34872,00

B2 Torsion with 30 degrees in wave propagation direction

Part	Segment	Element	Bridge girder [m]	Torsion [Nm]
End 1	1	1	0	1059600,00
		2	7,8125	1059300,00
		3	15,625	1058700,00
		4	23,4375	1057700,00
		5	31,25	1055900,00
		6	39,0625	1053100,00
	2	7	46,875	1049000,00
		8	54,6875	1043500,00
Beam 1	1	9	62,5	786840,00
		10	70,3125	786870,00
	2	11	78,125	788580,00
		12	93,75	794780,00
		13	109,375	800270,00
		14	125	801860,00
		15	140,625	797560,00
		16	156,25	786860,00
	3	17	171,875	775340,00
		18	179,6875	767160,00
Beam 2	1	19	187,5	641890,00
		20	195,3125	651370,00
	2	21	203,125	664840,00
		22	218,75	678230,00
		23	234,375	685170,00
		24	250	686150,00
		25	265,625	681910,00
		26	281,25	676090,00
	3	27	296,875	673550,00
		28	304,6875	673100,00
End 2	1	29	312,5	1123400,00
		30	320,3125	1130400,00
	2	31	328,125	1135600,00
		32	335,9375	1139200,00
		33	343,75	1141400,00
		34	351,5625	1142600,00
		35	359,375	1143200,00
		36	367,1875	1143500,00

B3 Shear forces in y- and z-direction with 30 degrees in wave propagation direction

Y – direction	
Bridge girder [m]	**Shear [N]**
0	1064,30
7,8125	1064,40
15,625	3201,60
23,4375	5246,10
31,25	7197,80
39,0625	9065,00
46,875	10852,00
54,6875	12748,00
62,5	14741,00
70,3125	35347,00
78,125	34687,00
93,75	32967,00
109,375	31674,00
125	30250,00
140,625	28718,00
156,25	-27306,00
171,875	26879,00
179,6875	27643,00
187,5	27632,00
195,3125	35365,00
203,125	35276,00
218,75	34643,00
234,375	34445,00
250	33986,00
265,625	33390,00
281,25	32602,00
296,875	31646,00
304,6875	31864,00
312,5	32121,00
320,3125	22581,00
328,125	19374,00
335,9375	16372,00
343,75	13588,00
351,5625	10717,00
359,375	7765,80
367,1875	4724,60
375	-1625,50

Z – direction	
Bridge girder [m]	**Shear [N]**
0	25232000,00
7,8125	25232000,00
15,625	24004000,00
23,4375	22777000,00
31,25	21549000,00
39,0625	20320000,00
46,875	19089000,00
54,6875	17713000,00
62,5	16190000,00
70,3125	14938000,00
78,125	14300000,00
93,75	13553000,00
109,375	12392000,00
125	10677000,00
140,625	8484500,00
156,25	5913700,00
171,875	3077700,00
179,6875	740320,00
187,5	-1090200,00
195,3125	1075800,00
203,125	-719060,00
218,75	-3052600,00
234,375	-5881700,00
250	-8455800,00
265,625	-10660000,00
281,25	-12394000,00
296,875	-13573000,00
304,6875	-14323000,00
312,5	-14963000,00
320,3125	-16161000,00
328,125	-17680000,00
335,9375	-19055000,00
343,75	-20285000,00
351,5625	-21513000,00
359,375	-22740000,00
367,1875	-23967000,00
375	-25195000,00

C1 Moment about y- and z-axis with 0 degrees in wave propagation direction

Y – axis	
Bridge girder [m]	**Moment [Nm]**
0	207,34
7,8125	197380000,00
15,625	385160000,00
23,4375	563350000,00
31,25	731940000,00
39,0625	890930000,00
46,875	1040300000,00
54,6875	1178900000,00
62,5	1305500000,00
70,3125	-774980000,00
78,125	-663410000,00
93,75	-451710000,00
109,375	-258000000,00
125	-91047000,00
140,625	45912000,00
156,25	136500000,00
171,875	183990000,00
179,6875	189970000,00
187,5	182440000,00
195,3125	190740000,00
203,125	185650000,00
218,75	138830000,00
234,375	47426000,00
250	-91478000,00
265,625	-257340000,00
281,25	-449800000,00
296,875	-660270000,00
304,6875	-771270000,00
312,5	-887560000,00
320,3125	1175300000,00
328,125	1037200000,00
335,9375	888360000,00
343,75	729870000,00
351,5625	561790000,00
359,375	384120000,00
367,1875	196850000,00
375	-153,27

Z – axis	
Bridge girder [m]	**Moment [Nm]**
0	22,03
7,8125	18,43
15,625	17,09
23,4375	35,60
31,25	66,24
39,0625	108,03
46,875	157,69
54,6875	214,99
62,5	280,57
70,3125	-973,00
78,125	-990,40
93,75	-927,23
109,375	-1073,00
125	-1223,90
140,625	-1377,60
156,25	-1560,40
171,875	-1752,90
179,6875	-2009,10
187,5	-2108,40
195,3125	-1879,60
203,125	-1775,80
218,75	-1414,30
234,375	-1244,80
250	-1076,50
265,625	-936,91
281,25	-850,38
296,875	-865,04
304,6875	-1051,60
312,5	-1084,60
320,3125	-232,63
328,125	-178,24
335,9375	-129,84
343,75	-86,69
351,5625	-51,23
359,375	-26,57
367,1875	-20,33
375	21,49

C2 Torsion with 0 degrees in wave propagation direction

Part	Segment	Element	Bridge girder [m]	Torsion [Nm]
End 1	1	1	0	576,74
		2	7,8125	576,43
		3	15,625	575,77
		4	23,4375	574,66
		5	31,25	572,95
		6	39,0625	570,46
	2	7	46,875	566,30
		8	54,6875	561,70
Beam 1	1	9	62,5	344,73
		10	70,3125	343,44
	2	11	78,125	349,84
		12	93,75	348,49
		13	109,375	345,14
		14	125	338,66
		15	140,625	328,16
		16	156,25	313,51
	3	17	171,875	292,26
		18	179,6875	282,18
Beam 2	1	19	187,5	241,77
		20	195,3125	251,24
	2	21	203,125	258,03
		22	218,75	269,84
		23	234,375	279,95
		24	250	286,87
		25	265,625	291,58
		26	281,25	298,94
	3	27	296,875	305,55
		28	304,6875	309,37
End 2	1	29	312,5	556,90
		30	320,3125	560,42
	2	31	328,125	563,68
		32	335,9375	565,46
		33	343,75	566,67
		34	351,5625	567,46
		35	359,375	567,94
		36	367,1875	568,18

C3 Shear forces in y- and z-direction with 0 degrees in wave propagation direction

Y – direction	
Bridge girder [m]	**Shear [N]**
0	1,60
7,8125	1,60
15,625	2,53
23,4375	3,39
31,25	4,18
39,0625	4,91
46,875	5,59
54,6875	6,36
62,5	-7,48
70,3125	-99,01
78,125	-98,78
93,75	-34,96
109,375	-35,07
125	-35,32
140,625	-35,44
156,25	-35,41
171,875	-35,25
179,6875	-99,15
187,5	-99,52
195,3125	-101,73
203,125	-101,58
218,75	-37,70
234,375	-37,38
250	-36,99
265,625	-36,43
281,25	-35,72
296,875	-34,94
304,6875	-98,71
312,5	-98,79
320,3125	7,96
328,125	7,14
335,9375	6,39
343,75	5,72
351,5625	5,01
359,375	4,23
367,1875	3,39
375	2,47

Z - direction	
Bridge girder [m]	**Shear [N]**
0	25264000,00
7,8125	25264000,00
15,625	24036000,00
23,4375	22808000,00
31,25	21580000,00
39,0625	20350000,00
46,875	19117000,00
54,6875	17739000,00
62,5	16214000,00
70,3125	14934000,00
78,125	14296000,00
93,75	13560000,00
109,375	12409000,00
125	10703000,00
140,625	8517000,00
156,25	5948500,00
171,875	3111600,00
179,6875	772730,00
187,5	-1121300,00
195,3125	1095900,00
203,125	-735770,00
218,75	-3061400,00
234,375	-5884500,00
250	-8457400,00
265,625	-10669000,00
281,25	-12408000,00
296,875	-13592000,00
304,6875	-14346000,00
312,5	-14988000,00
320,3125	-16158000,00
328,125	-17679000,00
335,9375	-19055000,00
343,75	-20286000,00
351,5625	-21515000,00
359,375	-22742000,00
367,1875	-23969000,00
375	-25197000,00